HAL
open science

Experimental investigation of screech by an underexpanded supersonic jet with forward flight effect

Benoît André, Thomas Castelain, Christophe Bailly, Daniel Juvé

To cite this version:

Benoît André, Thomas Castelain, Christophe Bailly, Daniel Juvé. Experimental investigation of screech by an underexpanded supersonic jet with forward flight effect. 10ème Congrès Français d'Acoustique, Apr 2010, Lyon, France. hal-00550554

HAL Id: hal-00550554

https://hal.science/hal-00550554v1

Submitted on 28 Dec 2010

HAL is a multi-disciplinary open access archive for the deposit and dissemination of scientific research documents, whether they are published or not. The documents may come from teaching and research institutions in France or abroad, or from public or private research centers.

L'archive ouverte pluridisciplinaire **HAL**, est destinée au dépôt et à la diffusion de documents scientifiques de niveau recherche, publiés ou non, émanant des établissements d'enseignement et de recherche français ou étrangers, des laboratoires publics ou privés.

10ème Congrès Français d'Acoustique

Lyon, 12-16 Avril 2010

Experimental investigation of screech by an underexpanded supersonic jet with forward flight effect

Benoît André[1], Thomas Castelain[1], Christophe Bailly[1], Daniel Juvé[1]

[1] Laboratoire de Mécanique des Fluides et d'Acoustique, École Centrale de Lyon,

36 avenue Guy de Collongues, 69134 Écully CEDEX, France, Email : benoit.andre@ec-lyon.fr

A coaxial supersonic facility has been upgraded in the anechoic room of the Centre Acoustique (LMFA, Ecole Centrale de Lyon) to reproduce a supersonic fan flow in forward flight. This paper first presents this new facility and some validation tests. A and B screech modes are characterized. Near-field microphones can well discriminate these two modes. A chaotic behaviour is found for mode B, which cannot be explained by mode switching. The effect of secondary flow on screech is essentially a decrease in frequency. Frequency jumps and hysteresis have also been observed with flight speed.

1 Introduction

In modern engines, the exit flow is separated into a hot supersonic core flow and a cold supersonic fan flow by two nozzles for cruise conditions. In the latter, there occurs a pressure mismatch at the exit which entails the generation of a shock cell structure in the jet. The design of the next generation aircraft will demand additional efforts on the reduction of shock-associated noise [2, 7]. Weight reduction concerns lead to introduce light composite materials in the fuselage of the next Airbus A350 or Boeing Dreamliner B787 whose sound transmission loss are weaker than in the case of traditional materials. Shock-associated noise is then the stronger contributor for the aft cabin interior noise. It can be divided into a broadband component and a narrow band one, the so-called screech.

Ever since the pioneering work of Powell [11], screech has been explained as a feedback process. The main idea is that aerodynamic disturbances originating from the nozzle lip interact with the shock cell pattern as they grow whilst being convected downstream, this interaction producing acoustic waves. The latter propagate then in the upstream direction and excite the shear layer near the nozzle lips, which produces disturbances and closes the feedback loop. Many investigators have contributed to the understanding of the screech generation process and have provided means how to annihilate it [4, 5, 10, 12, 13]. For circular jets, it is known since Powell [11] that the screech has a modal behaviour as the nozzle pressure ratio –NPR – varies. The modes or stages were called A, B, C and D and are observable by jumps in the screech frequency curve as the NPR varies. Merle [9] noted that mode A could be broke down into A1 and A2. The modes are otherwise characterized by a distinctive oscillation pattern for the aerodynamic perturbations as well as for the acoustic waves. For example, A is a symmetrical mode while B is a sinuous one. Finally, mode instabilities have been noticed [8, 9, 12].

The paper is organized as follows. The coaxial facility and instrumentation are provided in section 2. Section 3 deals with acoustic results on screech. Concluding remarks are finally given in section 4.

2 Experimental apparatus

2.1 The dual-stream wind tunnel facility

The jet facility of Centre Acoustique - LMFA UMR CNRS 5509 located at Ecole Centrale de Lyon has recently been used for single high Reynolds number subsonic jet studies [3, 6]. A major upgrade offers now the possibility to study coaxial supersonic jets. A dual-stream wind tunnel with a supersonic or primary duct may be embedded in a subsonic or secondary one as is sketched in Fig. 1. The flow in the first one originates from a Centac C60MX2-SH Ingersoll-Rand compressor using air previously dried by a Donaldson DV 5500 WP drier. The compressor can deliver a continuous mass flow rate of $1\,\mathrm{kg.s^{-1}}$. An electrically driven valve downstream of the compressor permits the regulation of the primary flow velocity by controlling the mass flow rate. After that, three electrical resistances, with a 64 kW maximal power, allow to heat the flow.
The flow in the subsonic duct is generated by an electronically controlled Neu LAK 4280A ventilator (2 bars pressure difference) delivering a nominal mass flow rate of $15\,\mathrm{kg.s^{-1}}$.

Downstream of the resistances, the tunnels enter the $10 \times 8 \times 8\,\mathrm{m}^3$ anechoic chamber of the LMFA. The supersonic duct then slips within the subsonic one thank to a flexible pipe. In the exit region of the wind tunnel, the two ducts are therefore coaxial. At the end of them are two contoured convergent axisymmetric nozzles. The primary duct is terminated by a $D_p = 38\,\mathrm{mm}$ diameter aluminium nozzle while the secondary nozzle diameter can be either $D_s = 76.5\,\mathrm{mm}$ or $D_s = 200\,\mathrm{mm}$, both being made out of resin. The lip thickness of the aluminium nozzle is 0.5 mm.

A calibration procedure permits to link secondary

flow velocity to ventilator rotation speed while the stagnation pressure and temperature of the supersonic duct are measured by total pressure and thermocouple probes as soon as it enters the anechoic chamber. The maximal Mach number of the secondary flow is 0.41 while the fully expanded Mach number M_j ranges up to 1.59, corresponding to a NPR of 4.17, for the supersonic nozzle. The NPR is defined as the ratio between the total pressure and the ambient pressure in the anechoic room.

Jet flow fields have been characterized in a subsonic regime prior to the acoustical measurements that constitute the core of the paper. A Pitot tube connected to a 2000 mm H_2O Furness manometer is used to measure the mean velocity in planes perpendicular to the nozzle exit plane. A unidirectional 55P11 Dantec hot wire is plugged into a CTA Dantec Streamline anemometer so as to measure turbulent velocity profiles. A thermocouple sensor is fixed on the Pitot tube. Manometer, anemometer and thermocouple output are connected to a NI PXI analyzer linked to a processor. The mean velocity profile are shown along with turbulence intensity in Fig. 2. It is visible that the jet is fully homogeneous in both jet cores. As for turbulence intensity, it is below 1 % within the jet cores and about 16-17 % in both shear layers. Although the operating condition of the primary duct is not representative of what it is meant to become, these measurements ensure that the coaxial wind tunnel does not suffer from a severe trouble.

2.2 Instrumentation

A conventional Z-type Schlieren system is used to visualize the global structure of the choked jet. It consists of a fibered continuous QTH light source whose adjustable electrical power ranges up to 250 W and of two $\lambda/8$, 107.95 mm diameter, 863.6 mm focal length parabolic mirrors. The off-axis use of the mirrors is limited to $2\,\alpha = 10°$ in order to reduce aberrations. A simple knife edge plays the role of the spatial filter. The Schlieren images have been recorded by a Phantom V12 CMOS camera, capable of 6 kHz frame rate at full frame size.

Far field acoustic measurements have been led using a quarter-of-inch microphone mounted on a frame rotating about the center of the coaxial nozzles in the exit plane at a distance of 1.7 m. Near field measurements have also been performed with two microphones set just upstream of the nozzle exit plane, in a vertical plane centered on the nozzle, one below the jet and the other above it. The microphones are of type B&K 4135 or B&K 4939 depending on the case, whose measured signals have been sampled at 102400 Hz using a NI PXI 5733 board.

3 Results

3.1 Screech noise

Screech tones have been a constant of virtually all measurements and will be dealt with in this section. To ensure that screech is the correct physical mechanism measured and that there is not some other feedback loop, it seemed necessary to investigate into the properties of the narrow band tone and to compare them with well-known screech characteristics in circular jets. The nozzle pressure ratio in the various acoustic measurements ranges from 1.58 to 3.21, all of which is below 1.89 generating a subsonic flow, then uninteresting here.

A decrease in screech frequency and a jump at some point were clearly noticed while continuously increasing the NPR, which is in accordance with the screech behaviour. The frequency jump betrays the modal feature of screech in circular jets, first addressed in Powell's pioneering work [11]. The separation between A and B modes occurred approximately at the expected NPR [12]. The directivity of the narrow band tone was also measured in a horizontal plane centered on the nozzle in 10° steps from $\theta = 30°$ (downstream) to $\theta = 130°$ (upstream), θ being the angle from the nozzle outlet axis to the microphone position. For each position, a narrow band spectrum was recorded, which permitted to compare the strengths of the various harmonics of the tone. It appeared that the fundamental tone was prominent in the upstream and downstream directions and that the first harmonic dominated at $\theta = 90°$. This is consistent with directivity properties of screech tones [10, 11].

To be more quantitative in the determination of the nature of the narrow band tone in the measurements, one can compare the measured frequencies of the fundamental tones with the predicted screech frequencies, by means of some analytical formulæ. Two different expressions are reported here. The first one was proposed by Powell [11] :

$$f_s = \frac{1}{3(\mathsf{NPR} - \mathsf{NPR_c})^{1/2}} \frac{a_\infty}{D_p} \quad \text{with} \quad \mathsf{NPR_c} = \left(\frac{\gamma+1}{2}\right)^{\gamma/(\gamma-1)}, \tag{1}$$

where f_s is the screech frequency, $\mathsf{NPR_c}$ the critical nozzle pressure ratio approaching 1.89 for air and a_∞ the speed of sound in ambient medium. The second estimation is given by Raman [13]

$$f_s = \frac{u_c}{s(1 + u_c/a_\infty)}, \tag{2}$$

where u_c is the convection velocity of turbulent structures in the shear layer of the jet, evaluated here at 70 % of the jet fully expanded velocity u_j, and s the shock cell spacing of the imperfectly expanded jet, measured from Schlieren visualizations. It is worth noting that these expressions do not account for the modal behaviour of screech tones. The result of this comparison for some operating conditions that will appear in the following is shown in Tab. 1. It is believed that the agreement between measured and computed frequency is acceptable, and it has to be noticed that the measured frequency lays in each case between the two predicted frequencies.

As a conclusion to this section, it seems reasonable to assume that the tone arising in the present study be indeed a screech tone and not a spurious reflection or any other artefact.

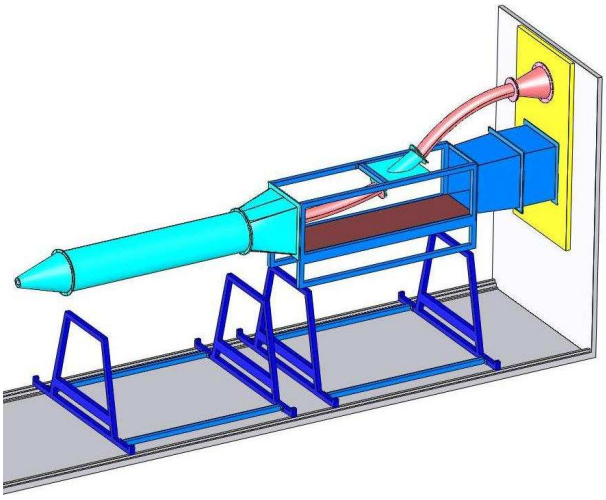

Figure 1: Sketch of the coaxial facility. Flows run to the left. The supersonic duct is in red, the subsonic one in blue.

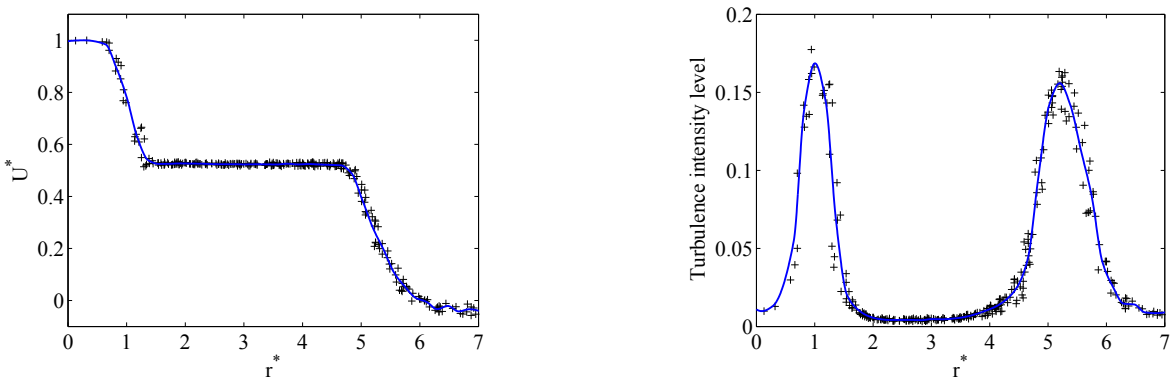

Figure 2: Left : mean velocity profile against radial position ; $U^* = U/U_p$ is the ratio of mean velocity to the primary jet exit velocity ($U_p = 163$ m.s^{-1}) and $r^* = r/r_p$ denotes the radial location divided by the primary nozzle radius. Right : turbulence intensity levels against r^*, computed by the ratio of RMS fluctuating velocity to the mean velocity difference between the two adjacent flows. The profiles are plotted from 291 measurement points uniformly distributed in a vertical plane $0.5\,D_p$ downstream of the exit. $D_s = 200$ mm.

NPR	measured frequency (Hz)	screech prediction from [11] (Hz)	error	screech prediction from [13] (Hz)	error
2.27	5669	4869	0.14	6463	0.14
2.54	3952	3719	0.06	4773	0.2

Table 1: Comparison between the measured frequency of fundamental narrow band tones and the predicted screech frequencies.

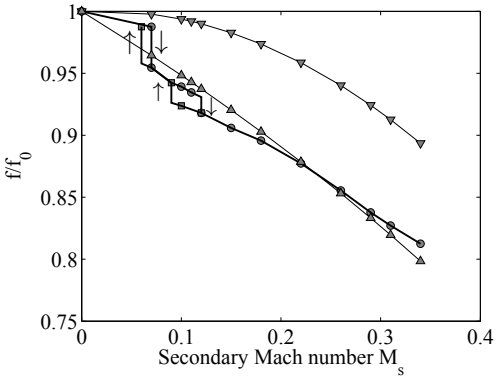

Figure 3: Variation of screech frequency f with the secondary Mach number M_s and comparison with analytical formulæ. NPR = 3.17. $D_s = 200$ mm. ▽ Bryce & Pinker [1], △ Tam [14]. ○ present study, increasing M_s, □ present study, decreasing M_s. f_0 is the computed or measured frequency without flight effect : ▽ and △ : 3588 Hz, present study 3210 Hz.

3.2 Screech modes

As already pointed out in section 3.1, screech has a modal behaviour. Two modes or stages are discernable in this NPR range : one of the two A mode and mode B. In this section, these modes are observed using near field microphones.

Time signals provided by two near field microphones are shown in Fig. 4 over a short interval. One striking feature visible here is the true sinusoid which denotes a strong screech tone. Also remarkable is the clearly defined relationship between the two measured signals at each NPR. At the lower one, two in-phase signals can be observed, which indicates a symmetric screech stage. Mode A is indeed a symmetric one. At the upper NPR, the signals obviously show an opposite phase relation which is consistent with an antisymmetric B mode. The literature distinguishes between several antisymmetrical stages but more microphones would be needed to investigate further in this direction.

One interesting feature is the behaviour of mode B. The steadiness of the microphone outputs for modes A and B are compared in Fig. 5 over the entire one second duration signal. It is found here that mode B is very unsteady, contrary to mode A. Few studies [9] pointed out the instability of mode B while others [8, 12] revealed the unsteadiness of mode D.

A time frequency analysis approach has been adopted to investigate into these instabilities. From the one second duration record displayed in Fig. 5, two particular sections have been selected to perform a Fourier analysis. Both extracts are 4096 signal values long or 0.04 s duration, which gives 25 Hz resolution spectra as output, which are displayed in Fig. 6. The main feature is that the fundamental screech frequency is the same in the two sections, equal to 3952 Hz (± 12.5 Hz). This ensures that the mentioned unsteadiness is not a mode switching and that for both extracts, mode B is observed. Furthermore, the narrow band sound pressure level (SPL) around the screech frequency increases much from the weak screech section to the strong one,

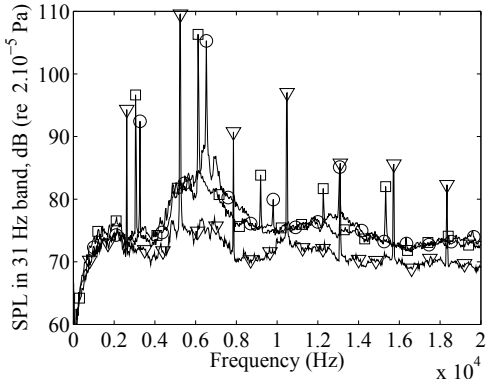

Figure 7: Effect of the secondary flow Mach number M_s on far field acoustic spectra. NPR = 3.17, $\theta = 90°$, $D_s = 200$ mm. ○ $M_s = 0$, □ $M_s = 0.07$, ▽ $M_s = 0.34$.

which correlates the time data displayed in Fig. 5 (right). It is also visible that the spectral energy is distributed differently in the two cases but it was found that the distribution is case dependent. Further input are needed to explain these instabilities.

3.3 Forward flight effect on screech

The influence of a secondary stream on screech is now considered. The evolution of acoustic spectra with an increasing secondary flow Mach number M_s is shown in Fig. 7. The screech amplitude is found to increase slightly, which is in general the case. The screech frequency consistently falls when the secondary flow strengthens. This can be explained by a simple argument in recalling the screech feedback loop. If one assumes that a secondary flow has little influence on the global features of the supersonic flow (inner part of the feedback loop), its major effect will then consist in lowering the effective speed of sound of acoustic waves propagating upstream (outer part of the loop). Looking back at Eq. (1) or Eq. (2), a decrease in the screech frequency is to be expected, which is indeed correlated by the experimental results. Tam [14] provides an analytical expression of the effect of forward flight on screech frequency consistent with this argument. Bryce & Pinker [1] propose a finer prediction in taking into account the increase of convective velocity of aerodynamic disturbances with M_s. Both are compared to the present experimental results, obtained by varying the secondary flow velocity and noting the screech fundamental frequency at each operating condition. In Fig. 3 is given the evolution with M_s of the non dimensioned screech frequency, *i.e.* the ratio of the screech frequency to the predicted or measured frequency with $M_s = 0$. The primary flow Mach number is fixed in this case, the NPR being equal to 3.17. Tam's formula sticks quite well to the experimental points but the trend seems more accurately predicted by Bryce & Pinker for larger M_s.

One striking feature of the experimental results, not accounted for by the theoretical models, is the presence of frequency jumps. This suggests mode switching, as mentioned by Tam [14] in the case of a supersonic screeching jet in forward flight. However, this behaviour cannot be directly explained by the evolution of screech

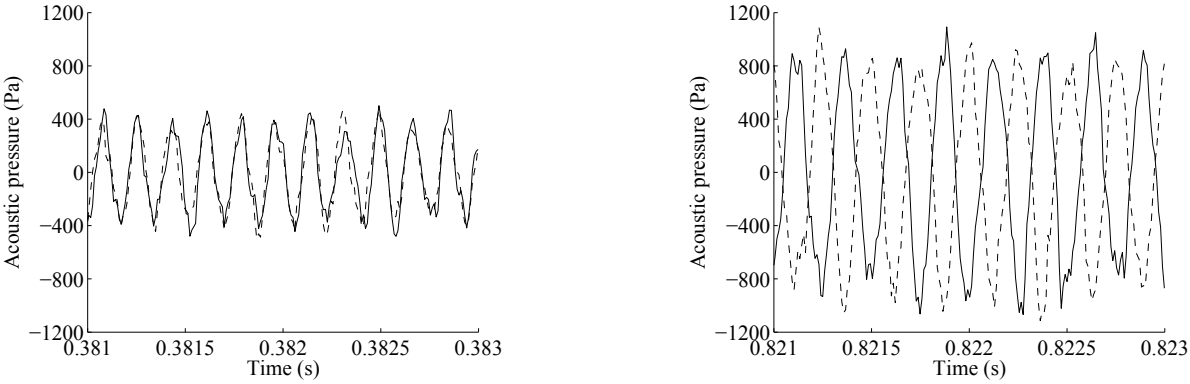

Figure 4: Time signals from two microphones located on either side of the nozzle (denoted by solid line and dashed line). Left, NPR = 2.27 and right, NPR = 2.54.

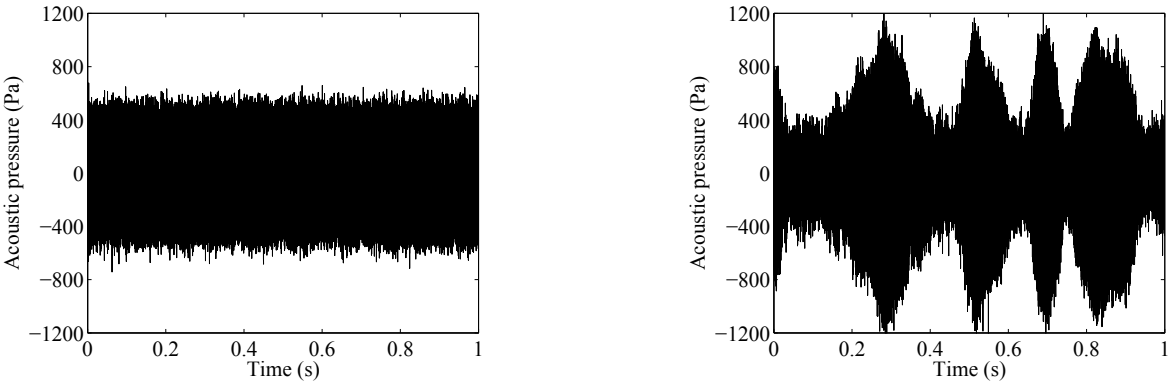

Figure 5: Time signals over one second recorded from one microphone located on the nozzle. Left, NPR = 2.27 and right, NPR = 2.54.

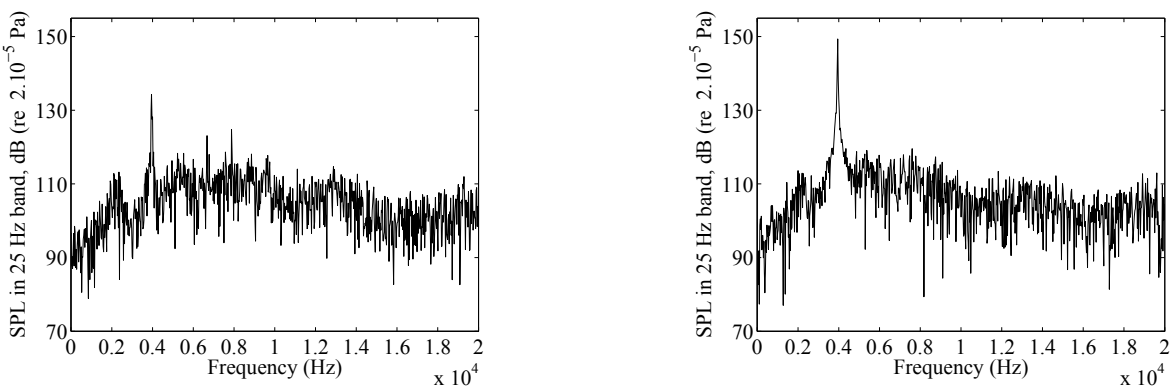

Figure 6: Time frequency analysis of the unsteadiness of mode B (see Fig. 5 right). NPR = 2.54. Left, sound pressure level (SPL) of a weak screech section from 0.046 s, 4096 values long. Right, SPL of a strong screech section from 0.84 s, 4096 values long.

frequency for single jets with NPR [12]. Complementary measurements of the acoustic field would then be necessary to investigate further into this phenomenon.

Moreover, a hysteretical behaviour of the frequency variations is visible in Fig. 3. A hysteretical behaviour with the velocity is known to occur for single jets. Still, to the authors' knowledge, the present phenomenon has not been reported on so far.

4 Conclusion

First acoustic results obtained in the upgraded jet facility of the Centre Acoustique (LMFA & Ecole Centrale de Lyon) have been presented in this work. The so-called A mode and B mode of screech have been investigated. It is shown that the signals from two opposite microphones are well in-phase and in opposite phase relation for modes A and B respectively. Mode B displays some chaotic variations which have been investigated by a time frequency analysis : no mode switching has been detected. A secondary flow let the screech frequency decrease with some jumps and a hysteretical phenomenon. The analytical formula of Bryce & Pinker [1] seems to predict well the evolution of the frequency if jumps are not considered.

This work is currently in progress. Detailed acoustic near field measurements should allow to gain some knowledge of the observed screech modes and to isolate the mode switching phenomena. Aerodynamical measurements made with use of Schlieren technique or Laser Doppler Velocimetry synchronized with acoustic ones should permit to link aerodynamical phenomena with acoustic emissions.

Acknowledgements

The authors would like to thank Emmanuel Jondeau, Jean-Michel Perrin and Pascal Souchotte for their technical support.

References

[1] Bryce, W. D., and Pinker, R. A. The noise from unheated supersonic jets in simulated flight. *AIAA Paper*, 77-1327 (1977).

[2] Calkins, F. T., Butler, G. W., and Mabe, J. H. Variable geometry chevrons for jet noise reduction. *AIAA Paper*, 2006-2546 (2006).

[3] Castelain, T., Sunyach, A., Juvé, D., and Béra, J. Jet-noise reduction by impinging microjets: An acoustic investigation testing microjet parameters. *AIAA Journal 46*, 5 (2008), 1081–1087.

[4] Davies, M. G., and Oldfield, D. E. S. Tones from a choked axisymmetric jet. i. cell structure, eddy velocity and source locations. *Acustica 12*, 4 (1962), 257–266.

[5] Davies, M. G., and Oldfield, D. E. S. Tones from a choked axisymmetric jet. II. the self excited loop and mode of oscillation. *Acustica 12*, 4 (1962), 267–277.

[6] Fleury, V., Bailly, C., Jondeau, E., Michard, M., and Juvé, D. Space-Time correlations in two subsonic jets using dual particle image velocimetry measurements. *AIAA Journal 46*, 10 (2008), 2498–2509.

[7] Huber, J., Sylla, A. A., Fleury, V., Bulté, J., Britchford, K., Laurendeau, E., and Long, D. Understanding and reduction of cruise jet noise at model and full scale. *AIAA Paper*, 2009-3382 (2009).

[8] Jothi, T. J. S., and Srinivasan, K. Role of initial conditions on noise from underexpanded pipe jets. *Physics of Fluids 21*, 6 (2009).

[9] Merle, M. Sur la fréquence des ondes émises par un jet d'air à grande vitesse. C. R. 243, Académie des sciences de Paris, 1956.

[10] Norum, T. D. Screech suppression in supersonic jets. *AIAA Journal 21*, 2 (1983), 235–240.

[11] Powell, A. On the mechanism of choked jet noise. *Proceedings of the Physical Society of London 66*, 408 (1953), 1039–1056.

[12] Powell, A., Umeda, Y., and Ishii, R. Observations of the oscillation modes of choked circular jets. *Journal of the Acoustical Society of America 92*, 5 (1992), 2823–2836.

[13] Raman, G. Supersonic jet screech: Half-century from powell to the present. *Journal of Sound and Vibration 225*, 3 (1999), 543–571.

[14] Tam, C. K. W. Jet noise generated by large-scale coherent motion. In *Aeroacoustics of flight vehicles : theory and practice ; vol 1 : Noise source*. H. H. Hubbard, 1991, pp. 311–390.